MassTransfer 2013

Data · February 2015

CITATIONS
0

READS
178

4 authors:

Serge Corbel
University of Lorraine
82 PUBLICATIONS **1,981** CITATIONS
SEE PROFILE

Nidhal Becheikh
University of Gabès
14 PUBLICATIONS **165** CITATIONS
SEE PROFILE

Thibault Roques-Carmes
French National Centre for Scientific Research
113 PUBLICATIONS **1,681** CITATIONS
SEE PROFILE

Orfan Zahraa
University of Lorraine
87 PUBLICATIONS **2,608** CITATIONS
SEE PROFILE

CHEMICAL ENGINEERING RESEARCH AND DESIGN XXX (2013) XXX–XXX

Contents lists available at ScienceDirect

Chemical Engineering Research and Design

journal homepage: www.elsevier.com/locate/cherd

Mass transfer measurements and modeling in a microchannel photocatalytic reactor

*Serge Corbel**, *Nidhal Becheikh*, *Thibault Roques-Carmes*, *Orfan Zahraa*
LRGP UMR 7274 CNRS – Université de Lorraine ENSIC, 1 rue Grandville, B.P. 20451, F-54001 Nancy Cedex, France

A B S T R A C T

The main objective of this paper was to evaluate the influence of mass transfer on the photocatalytic efficiency at a low flow rate in the order of several mL per hour. Several continuous flow microchannel reactors have been used to study the degradation of salicylic acid (SA) taken as a model pollutant. The photocatalytic degradation of salicylic acid, under UV illumination of 1.5 mW cm^{-2}, was assessed from the outlet concentration measured by liquid chromatography HPLC. It was shown that the degradation of SA by UV was limited by mass transfer. Numerical simulations have allowed establishing a relationship of the Sherwood number valuable for all the microchannel geometries. Computational fluid dynamics with Comsol Multiphysics is useful for predicting the degradation yield for a given geometry of the microreactor. The best representation of the experimental data is obtained by introducing a kinetic law taking into account mass transfer limitation.

Keywords: Photocatalysis; Continuous-flow; Microreactor; Kinetic modeling; Mass transfer; Microstructuration; Simulation

1. Introduction

Traditionally, photochemical reactors have operated in batch mode. This configuration leads to a non-uniform distribution of UV light and a mass transfer limitation due to a slow diffusion. Among the possible solutions for intensification of photocatalytic reactions, there is the use of microreactors (Van Gerven et al., 2007). Microreactors with channel dimensions of a few hundred microns, enable optimum utilization of incident radiation (Georges et al., 2004) and larger surface to volume ratio compared to classic reactors. In the light of these advantages, there have been a number of developments in the area of flow-based photochemical microprocesses (Teekateerawej et al., 2006; Mills et al., 2007; He et al., 2010; Charles et al., 2012; Tsuchiya et al., 2012).

In spite of the many work on heat transfer and pressure drop in microchannels, the mass transfer studies remains very limited. Acosta et al. (1985) investigated experimentally the mass transport in narrow flow gaps with dimensions ranging between 0.2 and 0.5 mm at large Reynolds numbers (Re = 1300–22 000). Van Male et al. (2004) explored, numerically and experimentally, the mass transfer in a square microchannel. They reported a Sherwood correlation for the channel heated from topside under laminar plug-flow. To the best of our knowledge, only one study relates the mass transfer determination in a rectangular microchannel (Barlay Ergu et al., 2009). The authors studied experimentally the local mass transfer in a rectangular channel with a hydraulic diameter of 0.208 mm. The Sherwood number correlation was reported with a power of the Reynolds number equal to 0.28.

In line with this reasoning, we report the photocatalytic degradation of SA on deposited catalyst TiO_2 in two microchannel reactors. The main objective of this paper was to evaluate the influence of mass transfer on the photocatalytic efficiency at a low flow rate. For this purpose, we have simulated the degradation reaction, with the objective to establish a relationship of the Sherwood number valid for several geometries and flow rates.

Overall, in this research, photocatalysis degradation of SA in TiO_2/UV system was investigated by (i) finding the conversion yield at each flow rate, (ii) modeling with COMSOL Multiphysics, and (iii) investigating the influence of mass transfer coefficient with the hydrodynamics.

* *Corresponding author*. Tel.: +33 03 83 17 51 14.
E-mail address: serge.corbel@univ-lorraine.fr (S. Corbel).
Received 19 July 2013; Received in revised form 30 August 2013; Accepted 10 October 2013
0263-8762/$ – see front matter © 2013 The Institution of Chemical Engineers. Published by Elsevier B.V. All rights reserved.
http://dx.doi.org/10.1016/j.cherd.2013.10.011

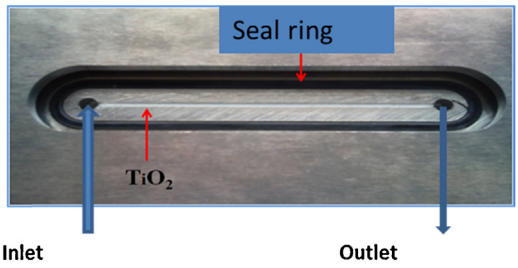

Fig. 1 – Photography of the microreactor with the central microchannel where is deposited the catalyst TiO_2.

2. Materials and methods

Several microchannel reactors have been tested (Corbel et al., 2008, 2011, 2012). They have been fabricated in inox by numerical machine. The top of the reactors was grooved with a microchannel. The micro-channels had a length of 70 mm. Only the results concerning two reactors are presented in this paper. Fig. 1 shows the design of the microreactor.

The two microchannel reactors characteristics are presented in Table 1. Both reactors display the same catalytic surface and roughly the specific surface κ (i.e., the surface area per unit of volume). All of them have a channel length of 70 mm.

The titanium dioxide samples were deposited on the micro-channel reactor (inner surface of the channel) according to the procedure of Furman et al. (2007). An aqueous suspension of TiO_2 Degussa P25 (Evonik) of 4 g/L at pH 3 was poured on the channel and the excess removed. The wetted channel was dried at 70 °C for 1 h. This coating process was repeated several times. After rinsing under running distilled water in order to remove loose particles, the amount of deposit was determined by weighing the dried reactor before and after the deposition. This method leads to a coating thickness of $5 \pm 1\,\mu m$ (determined by profilometry) and a surface load of $2.3 \pm 0.3\,mg/cm^2$. This value is generally required for complete light absorption (Ould-Mame et al., 2000; Zahraa et al., 1999). The photoreactor is a self-constructed microreactor with fluorescent lamp ($\lambda_{max} = 365$ nm). The microchannel is closed to the UV lamp so that the incident light power is $1.5\,mW\,cm^{-2}$ at the surface of the catalyst, i.e., the level of the bottom of the channel (Fig. 2). The measure was performed with an UV radiometer.

Salicylic acid (SA) solution ($10\,mg\,L^{-1}$) was injected by means of a syringe pump through the microreactor at a constant inlet flow rate between 2.5 and 20 mL/h. During the residence time, SA is adsorbed on TiO_2, which may result in a decrease of the solution concentration. To take into account of this effect, we carried out the photodegradation reaction after flowing SA in the microreactor for 1.5 h in the dark to reach the adsorption equilibrium. During the course of photocatalysis and irradiation, a sample is withdrawn after regular time intervals. The peak area on the chromatograms is converted to SA concentration using a linear calibration curve. It gives the output concentration of salicylic acid and then the conversion yield. For each reaction time, final results were averaged out of at least three independent experiments.

Fig. 2 – Experimental setup equipped with feed control consisting of a syringe pump system.

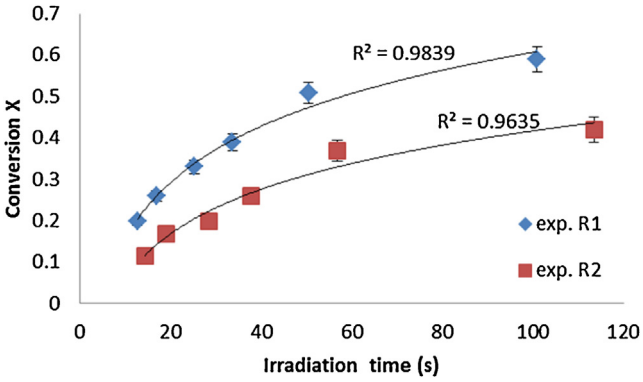

Fig. 3 – Experimental photocatalytic conversion yield of SA in microreactors R1 (depth = 0.5 mm) and R2 (depth = 0.75 mm) as a function of the irradiation time (lines are drawn for readability).

3. Photocatalytic activity

The reactors R1 and R2 have the same catalytic surface. In these experiments, the contact time τ equal to V/Q is adjusted by changing the flow rate Q. In this case, it is possible to compare the efficiency of the two reactors at the same contact time. Fig. 3 illustrates the variation of the conversion yield in the two reactors in function of irradiation time.

The conversion yields show a logarithmic growth with time to reach a constant level. The reactor with the smaller depth has the highest conversion. As they present almost the same catalytic surface S_c, the rate of degradation is improved by lowering the depth of the channel and by increasing the specific area κ. The apparent kinetic depends on the hydrodynamic and the boundary layer. This could be logically explained by a lower limitation by the mass transfer in reactor R1 and this aspect has been confirmed by simulation. A good agreement

Table 1 – Geometric characteristics for two microreactors with a channel length of 70 mm.

R_i	Width w (mm)	Depth h (mm)	Aspect ratio w/h	Volume V (mm^3)	Channel surface S_c(mm^2)	Spec. surface κ (mm^{-1})
R1	2	0.5	4	70.0	210	3.0
R2	1.5	0.75	2	78.7	210	2.7

Please cite this article in press as: Corbel, S., et al., Mass transfer measurements and modeling in a microchannel photocatalytic reactor. Chem. Eng. Res. Des. (2013), http://dx.doi.org/10.1016/j.cherd.2013.10.011

has been found between the models and experimental results. In the photocatalytic reaction, we estimate in agreement with (Shiraishi et al., 2006) that a recirculation mode may be beneficial owing to a reduction in the film-diffusional resistance.

4. Kinetics models generated by photonic excitation of the catalyst

A kinetic model (Mills et al., 2006) consists of the reversible adsorption–desorption reaction rate $k/k-1$, Eq. (1), of the organic pollutant followed by an oxido-reduction rate k_{LH} under UV light Eq. (2); this leads to the following mechanism:

$$SA\,(liquid) \rightarrow SA\,(ads) \quad (1)$$

$$SA(ads) \rightarrow k_{LH} + h\nu \rightarrow products \quad (2)$$

In this mechanism, it is assumed that a pseudo-steady state is reached and that the reaction (2) involves the oxidation of the organic SA by the hydroxyl radical generated by photonic excitation of the catalyst (Chen et al., 1994). The constant k_{LH} depends on the incident light intensity.

The pseudo-steady-state analysis of these reactions reveals a kinetic expression of the rate of removal r of the organic pollutant which can be well described by a Langmuir–Hinshelwood kinetic equation Eq. (3) (Mills et al., 2006; Hermann, 2010):

$$-r = \frac{k_{LH}K_{LH}C}{1 + K_{LH}C} \quad (3)$$

where k_{LH} and K_{LH} are the apparent rate and adsorption constants, respectively, and C is the reactant concentration in the bulk (mol m^{-3}). It is now recognized that the apparent rate constant is light-intensity dependant.

The reaction occurs on a thin film of titanium dioxide covering the inner surface of the channel. As it has been observed previously (Furman et al., 2007), this reaction is strongly influenced by the transfer of the reactant from the fluid bulk toward the catalyst surface. Such coupled effect of photocatalytic reaction and transfer limitation has been established in a previous work (Charles et al., 2011). The mass-flux toward the surface of the catalyst is equal to the chemical consumption of salicylic acid at the catalytic surface as expressed by the following Eq. (4):

$$-r = k_d(C - C_s) = \frac{k_{LH}K_{LH}C_s}{1 + K_{LH}C_s} \quad (4)$$

where C is the bulk concentration, k_d (m s^{-1}) the external mass transfer coefficient and K_{LH} (mol^{-1} m^3) the adsorption–desorption constant. The subscript s represents the value of the concentration at the photocatalyst surface. Furthermore, the surface concentration C_s depends on the bulk concentration and the external mass transfer. As the surface reaction is faster than the diffusion reaction, it can be assumed that the surface concentration C_s is negligible compared to C, so that the Eq. (4) becomes

$$-r = k_dC = \frac{kKC}{1 + KC} \quad (5)$$

At a given flow rate Q and during the residence time τ, the experimental degradation ratio of salicylic acid, is defined by the mean conversion ratio X. It represents the normalized variation of the salicylic acid concentration between the inlet and outlet of the reactor:

$$X(\tau) = \frac{C_0 - C_{out}}{C_0} \quad (6)$$

where C_0 (0.072 mol m^{-3}) and C_{out} are the inlet and outlet concentrations, respectively. The outlet concentration C_{out} is defined at a stationary state and varies with the flow rate. The value of the outlet concentration C_{out} is used to estimate the degradation ratio of salicylic acid by using Eq. (5). Every experiment is repeated at least three times, and the data presented below are the averages of the repeated results. The experimental uncertainty on the ratio X is less than 0.02 and we can deduce a maximum vertical error bar of 7% on the data series.

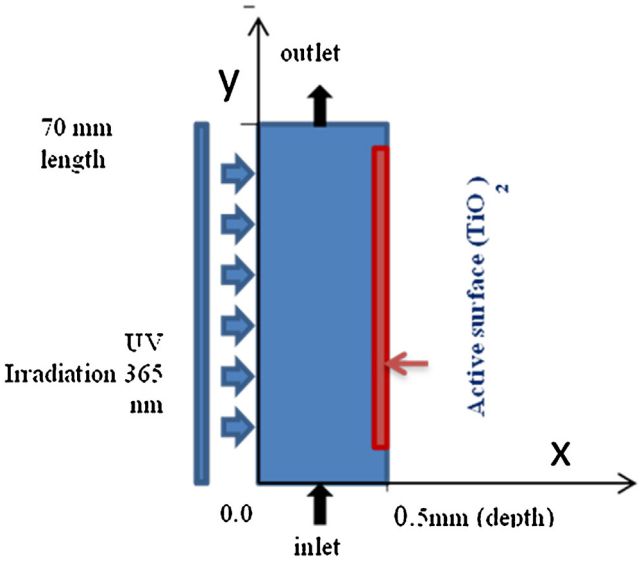

Fig. 4 – Schematic 2D model domain with the microchannel and the active catalytic surface TiO_2.

5. Modeling with COMSOL Multiphysics

The model takes into account the convection-diffusion phenomena occurring in a 2D domain which is coupled to salicylic acid transport to the reacting surface. The geometry of the model is a parallel plate reactor with an active surface where occurs the reaction. The contribution of the lateral walls (not represented) has been neglected and only the bottom of the channel whose orientation is perpendicular to the irradiation has been considered. Cross-side 2D geometry of the domain is shown in Fig. 4.

A Newtonian-incompressible flow has been adopted to simulate the aqueous flow of the solution through the channel. The governing equations are the well-known Navier–Stokes, whereas the surface concentration C_s is calculated by the material balance for the surface, including diffusion and the reaction rate expression:

$$\frac{\partial c_s}{\partial t} + (-D\nabla c_s) = r \quad (7)$$

where C_s is the surface concentration of SA in mol m^{-2} and r the surface reaction rate. In the model, the surface reaction rate r is considered as a negative boundary flux. We have simulated the reaction by considering two forms of the rate

expression. In a first step, we considered the reaction rate as the kinetics model of Langmuir–Hinshelwood (LH):

$$-r = \frac{k_{LH}K_{LH}C_s}{1 + K_{LH}C_s} \quad (8)$$

And in a second step, we introduced a reaction rate governed only by mass transfer from the bulk to the surface.

$$-r = k_d(C - C_s) \quad (9)$$

with k_d the external mass transfer constant, C and C_s the concentration in the bulk and the surface, respectively. The concentration C_s can be considered negligible in comparison with the C concentration in the bulk. Therefore, Eq. (9) could be approximated by

$$-r = k_d C \quad (10)$$

The coupling between the bulk and the surface is obtained as a boundary condition in the bulk's mass balance. This condition sets the flux of C at the boundary equal to the rate of the surface reaction.

The transport in the bulk of the channel is described by a convection–diffusion equation:

$$\frac{\partial c}{\partial t} + \nabla \cdot (-D\nabla c + cu) = 0 \quad (11)$$

In the above equation, D denotes the isotropic diffusion coefficient of SA in aqueous solution, and $u(x,y)$ denotes the flow velocity. In this case the velocity in the perpendicular direction x equals 0 while the velocity in the parallel direction y of the active surface has a Gaussian distribution due to laminar flow between two parallel plates. Moreover, during the meshing step, care is taken in order to have a large number of fine elements along the active surface and the total number of elements for a complete triangular mesh is 158 570.

5.1. *Comparison of the two models*

For a given geometry and an inlet concentration of $0.072\,mol\,m^{-3}$, the apparent kinetics constant ($k = 4.5 \times 10^{-7}\,mol\,m^{-2}\,s^{-1}$) and adsorption constant ($K = 40\,m^3\,mol^{-1}$) have been found in a previous work (Corbel et al., 2012). They allow calculating for each flow rate the outlet concentration C_{out} and the corresponding yield X. The average concentration C_{out} is calculated by integrating the concentration on the outlet border of the domain with an average operator. The diffusivity of SA is supposed to be isotropic and equal to $9.8 \times 10^{-10}\,m^2\,s^{-1}$ (Delgado, 2007). Fig. 5 shows the calculated and experimental conversion ratios as a function of the flow rate for the two models: Langmuir–Hinshelwood (sim LH) and mass transfer (sim transf.).

As expected, the conversion decreases with the flow rate which corresponds to a shorter contact time in the microchannel. At low flow rate, the two models describe correctly the experimental data, but they diverge at higher flow rates. By using the LH model, we observe a significant disagreement between the model and the experimental data. This effect illustrates the difficulty to choose correctly the couple of constants (k, K) of the LH model. On the opposite, when the model takes into account the mass transfer, a better agreement is now observed. Indeed, the variation of the mass

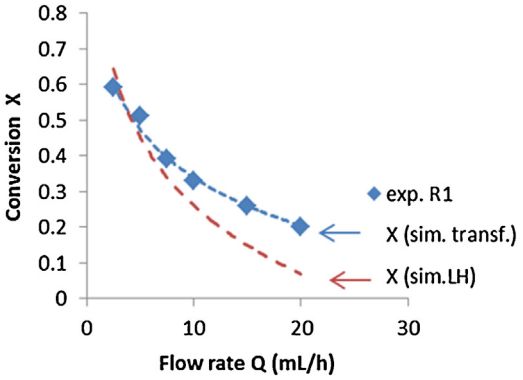

Fig. 5 – Comparison of the two models (kinetics model of LH and mass-transfer model) with experimental data for the reactor R1.

Table 2 – Values of mass transfer k_d obtained from the simulation by COMSOL and the deduced values of the Sherwood numbers in the case of reactor R1.

Q (mL/h)	*Re*	k_d simul (m/s)	$Sh = dh^*k_d/Dm$
2.5	0.6	6.3×10^{-6}	5.14
7.5	1.7	1.03×10^{-5}	8.41
10	2.2	1.10×10^{-5}	8.98
15	3.3	1.20×10^{-5}	9.80
20	4.4	1.15×10^{-5}	9.39

transfer with the flow rate influences the kinetics. In these conditions the model with diffusion and mass transfer seems more convenient. In the photocatalytic reaction, however, we estimate in agreement with (Shiraishi et al., 2006) that a recirculation mode may be beneficial owing to a reduction in the film-diffusional resistance. In addition, we verified by simulation the effect of the mass transfer by introducing baffles in half the depth of the microchannel. This causes a decrease of the output concentration and a significant increase of the conversion rate of the pollutant.

5.2. *Determination of the Sherwood number by simulation*

Using the COMSOL Multiphysics software, we took a kinetic law of degradation following an external mass transfer rule as described by Eq. (5) comprising the coefficient k_d. For a given flow, we can find the parameter k_d by fitting the conversion of experimental and simulated data. In the CFD simulation, only one parameters is unknown, namely k_d. To fit the experimental data to the model we use the following calculation scheme. At first, we fix the value of k_d. The resulting model value of conversion is then compared to the experimental degradation ratio at a given flow rate. The value of k_d is modified in such a way that the difference between the numerical solution and the experiment is minimal. Tables 2 and 3 give the values of k_d deduced from the simulation at each flow rate and the cor-

Table 3 – Values of mass transfer k_d obtained from the simulation by COMSOL and the deduced values of the Sherwood numbers in the case of reactor R2.

Q (mL/h)	*Re*	k_d simul (m/s)	$Sh = dh^*k_d/Dm$
2.5	0.6	5.5×10^{-6}	5.61
7.5	1.8	9.0×10^{-6}	9.18
10	2.5	8.3×10^{-6}	8.52
15	3.7	1.05×10^{-5}	10.71

Please cite this article in press as: Corbel, S., et al., Mass transfer measurements and modeling in a microchannel photocatalytic reactor. Chem. Eng. Res. Des. (2013), http://dx.doi.org/10.1016/j.cherd.2013.10.011

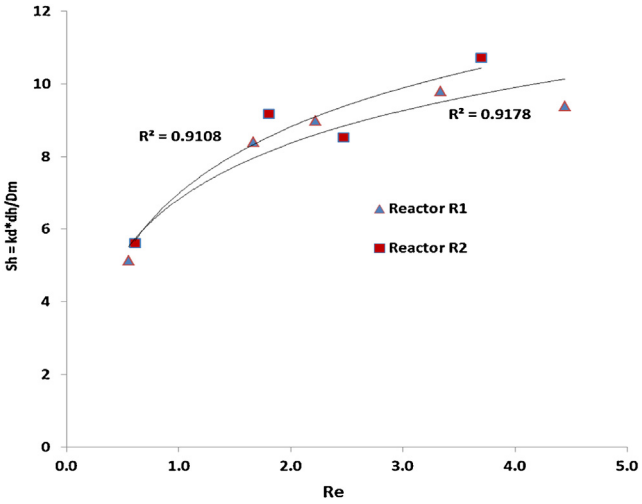

Fig. 6 – Sherwood number variation as a function of flow rate obtained from simulation and optimization of k_d in the case of reactors R1 and R2.

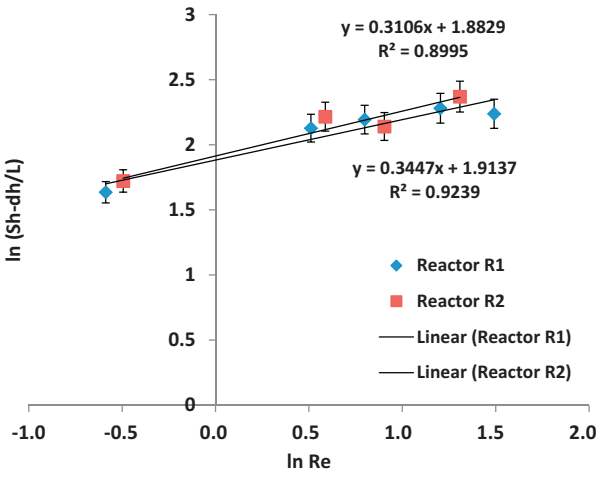

Fig. 7 – Linearization for finding the power values α and β in the case of reactors R1 and R2.

responding calculated values of the Sherwood number *Sh* for the reactors R1 and R2, respectively.

Fig. 6 shows the evolution of the Sherwood number with the Reynolds number. It increases with the flow rate and stabilizes for *Re* larger than 2. The trend is similar to that described by Barlay Ergu et al. (2009) for the mass transfer coefficient in rectangular microchannel, and by Chen et al. (2000) for the mass transfer coefficient of benzoic acid into water during the photocatalytic degradation inside a circular macro-reactor with immobilized titania oxide. All the former studies illustrate that the Sherwood number, or the mass transfer coefficient, increases (less mass transfer resistance) with increasing circulating flow rate. This causes a decrease of the output concentration and a significant increase of the conversion rate of the pollutant.

6. Correlation of the Sherwood with Reynolds and Schmitt numbers

We hypothesized that the number of Sherwood followed a law of the type:

$$Sh = \frac{d_h}{L} + Re^{\alpha} Sc^{\beta} \quad (12)$$

with d_h the hydraulic diameter, *L* the length of the microchannel, *Re* the Reynolds number and *Sc* the Schmidt number. The Schmidt number is calculated using $Sc = \mu/\rho D$, with μ and ρ the viscosity and the density of the solution, respectively.

The coefficients α and β were determined by linearization of Eq. (12), and the values are determined from the slope and intercept point, respectively. Fig. 7 shows the linearization, and the values found: $\alpha = 0.31$ for R1 and $\alpha = 0.34$ for the reactor R2. These curves can be used to deduce the value of the exponent β of the Schmidt number: $\beta = 0.27$ and $\beta = 0.28$ for R1 and R2, respectively. The obtained power law values of the Reynolds number α are comparable with that of about 0.26–0.32 already reported for a similar microchannel system (Barlay Ergu et al., 2009). In addition, the power exponents are in perfect agreement with the exponent corresponding to the Graetz–Leveque laminar flow conditions inside a membrane ($\alpha = 0.33$) (Van den Berg et al., 1989). The power values of the Schmidt number β agree with the results of Barlay Ergu et al. (2009) who found a power exponent of 1/3 and also to the Graetz–Leveque exponent given as 0.33.

The knowledge of the mass transfer coefficients with the flow rate allows us defining a law of the Sherwood number for a given geometry of the micro-channel reactor.

7. Conclusion

The degradation of SA was tested in different geometric configurations of the microreactors. It has been found that the microreactor with the smallest depth is the best configuration. This is in relation with the mass transfer toward the catalytic surface. The simulation of the degradation, taken into account the diffusion and the mass transfer toward the catalyst, shows an important concentration gradient. The best representation of the experimental data was obtained by introducing a kinetic law governed by mass transfer. By adjustment of the conversion yield, we have simulated the conversion yield at each flow rate. The simulation has allowed defining a correlation of the Sherwood number with the flow rate. The following expression was obtained: $Sh = dh/L + Re^{0.3}Sc^{0.3}$. This correlation defines a mass transfer coefficient that can adequately describe the experimental results in an area corresponding to the Reynolds number between 1 and 4.

Acknowledgments

This work was funded by 'Région de Lorraine'.

References

Acosta, R.E., Muller, R.H., Tobias, C.W., 1985. Transport processes in narrow (capillary) channels. AIChE J. 31, 473–482.

Barlay Ergu, O., Sara, O.N., Yapıcı, S., Arzutug, M.E., 2009. Pressure drop and point mass transfer in a rectangular microchannel. Int. Commun. Heat Mass Transfer 36, 618–623.

Charles, G., Roques-Carmes, T., Becheikh, N., Falk, L., Commenge, J.-M., Corbel, S., 2011. Determination of kinetic constants of a photocatalytic reaction in micro-channel reactors in the presence of mass-transfer limitation and axial dispersion. J. Photochem. Photobiol. A: Chem. 223, 202–211.

Charles, G., Roques-Carmes, T., Becheikh, N., Falk, L., Corbel, S., 2012. Impact of the design and the materials of rectangular micro-channel reactors on the photocatalytic decomposition of organic pollutant. Green Process. Synth. 1, 363–374.

Chen, D., Li, F., Ray, A.K., 2000. Effect of mass transfer and catalyst layer thickness on photocatalytic reaction. AIChE J. 46, 1034–1044.

Chen, H.Y., Zahraa, O., Bouchy, M., Thomas, F., Bottero, J.Y., 1994. Adsorption properties of TiO_2 related to the photocatalytic degradation of organic contaminants in water. J. Photochem. Photobiol. A: Chem. 85, 179–186.

Corbel, S., Charles, G., Becheikh, N., Roques-Carmes, T., Zahraa, O., 2012. Modelling and design of microchannel reactor for photocatalysis. Virtual Phys. Prototyping, 1–8, http://dx.doi.org/10.1080/17452759.2012.708837, i-First article (2012).

Corbel, S., Dufaud, O., Roques-Carmes, T., 2011. Material for stereolithography. In: Bartolo, P.J. (Ed.), Stereolithography: Materials, Processes and Applications. Springer-Verlag, New York, pp. 141–159.

Corbel, S., Evenou, F., Baros, F., Martinet, N., Donner, M., Carré, M-C., 2008. Micro-structured reactors designed by stereolithography and characterized by fluorescent probes. Int. J. Photoenergy, 1–7 (Article ID 757510).

Delgado, J.M.P.Q., 2007. J. Phase Equilib. Diffus. 28, 427–432.

Furman, M., Corbel, S., Le Gall, H., Zahraa, O., Bouchy, M., 2007. Influence of the geometry of a monolithic support on the efficiency of photocatalyst for air cleaning. Chem. Eng. Sci. 62, 5312–5316.

Georges, R., Meyer, S., Kreisel, G., 2004. Photocatalysis in microreactors. J. Photochem. Photobiol. A: Chem. 167, 95–99.

He, Z., Li, Y., Zhang, Q., Wang, H., 2010. Capillary microchannel-based microreactors with highly durable ZnO/TiO_2 nanorod arrays for rapid, high efficiency and continuous-flow photocatalysis. Appl. Catal. B: Environ. 93, 376–382.

Hermann, J.M., 2010. Photocatalysis fundamentals revisited to avoid several misconceptions. Appl. Catal. B: Environ. 99 (3–4), 461–468.

Mills, A., Wang, J., Ollis, D.F., 2006. Dependence of the kinetics of liquid-phase photocatalyzed reactions on oxygen concentration and light intensity. J. Catal. 243, 1–6.

Mills, P.L., Quiram, D.J., Ryley, J.F., 2007. Microreactor technology and process miniaturization for catalytic reactions—a perspective on recent developments and emerging technologies. Chem. Eng. Sci. 62, 6992–7010.

Ould-Mame, S.M., Zahraa, O., Bouchy, M., 2000. Photocatalytic degradation of salicylic acid on fixed TiO_2 – kinetic studies. Int. J. Photoenergy 2, 59–66.

Shiraishi, F., Nagano, M., Wang, S., 2006. Characterization of a photocatalytic reaction in a continuous-flow recirculation reactor system. J. Chem. Technol. Biotechnol. 81, 1039–1048.

Teekateerawej, S., Nishino, J., Nosaka, Y., 2006. Design and evaluation of photocatalytic micro-channel reactors using TiO_2-coated porous ceramics. J. Photochem. Photobiol. A: Chem. 179, 263–268.

Tsuchiya, N., Kuwabara, K., Hidaka, A., Oda, K., Katayama, K., 2012. Reaction kinetics of dye decomposition processes monitored inside a photocatalytic microreactor. Phys. Chem. Chem. Phys. 14, 4734–4741.

Van den Berg, G.B., Racz, I.G., Smolders, C.A., 1989. Mass transfer coefficients in cross-flow ultrafiltration. J. Membr. Sci. 47, 25–51.

Van Gerven, T., Mul, G., Moulijn, J., Stankiewicz, A., 2007. A review of intensification of photocatalytic processes. Chem. Eng. Process. 46, 781–789.

Van Male, P., de Croon, M.H.J.M., Tiggelaar, R.M., van den Berg, A., Schouten, J.C., 2004. Heat and mass transfer in a square microchannel with asymmetric heating. Int. J. Heat Mass Transfer 47, 87–99.

Zahraa, O., Dorion, C., Ould-Mame, S.M., Bouchy, M., 1999. Titanium dioxyde deposit films for photocatalytic studies of water pollutants. J. Adv. Oxid. Technol. 4, 40–46.

Please cite this article in press as: Corbel, S., et al., Mass transfer measurements and modeling in a microchannel photocatalytic reactor. Chem. Eng. Res. Des. (2013), http://dx.doi.org/10.1016/j.cherd.2013.10.011